**ISSN 1454 - 8003**
**Proceedings of 2017 International Conference on Hydraulics and Pneumatics - HERVEX**
*November 8-10, Băile Govora, Romania*

# CONTROL CONCEPT FOR A NOVEL INTEGRATED PRESSURE BOOSTER

**Stephan MERKELBACH[1], Olivier REINERTZ[2], Hubertus MURRENHOFF[3]**

[1] RWTH Aachen University, Institute for Fluid Power Drives and Controls (IFAS), stephan.merkelbach@ifas.rwth-aachen.de

[2] RWTH Aachen University, Institute for Fluid Power Drives and Controls (IFAS), olivier.reinertz@ifas.rwth-aachen.de

[3] RWTH Aachen University, Institute for Fluid Power Drives and Controls (IFAS), post@ifas.rwth-aachen.de

***Abstract:*** *The paper proposes a novel concept for pressure boosters based on rotational equipment. Instead of double piston boosters as they are common in industrial applications today, the proposed concept is based on a pneumatic radial piston motor. During one cycle, all cylinder chambers act as actuator and compressor as well. The paper shows a mathematical model of the cycle and its simulative implementation. A control concept using fast switching valves is proposed. To evaluate the efficiency, a parameter variation is undertaken. This includes the number and size of the pistons as well as pressure levels for input and output respectively. The thermodynamic concept of exergy is used to compare the different system configurations.*

***Keywords****: Pneumatics, Pressure Booster, Energy Efficiency, Simulation*

## 1. Introduction

Pneumatic drives are used in a great variety of applications, especially in manufacturing and process engineering. Since compressed air is an expensive form of energy, recent developments show a tendency to lower the overall system pressure in compressed air systems. This improvement should lead to higher efficiency in the compressor while larger drives are needed to provide equivalent driving forces [1]. On the other hand, some applications require compact drives and therefore a higher driving pressure. To ensure the applicability of these drives while maintaining the energy efficiency, a suitable option is to implement pressure boosters. Current concepts for pressure boosters feature double piston linear transformers which have a limited efficiency. To enhance the efficiency of pneumatic transformers, the paper proposes a novel concept based on a rotating unit. The concept consists of a radial piston motor which is used in a combined cycle as motor and compressor to boost the pressure.

## 2. Working principle of the novel booster concept

Pressure transducers based on rotational units have been around in hydraulics for several years. So called hydro transformers built from a separate pump and hydraulic motor are used for energy recovery in many different applications (see e.g. [2]). On the other hand, there are concepts using only one integrated rotational unit which serves as a combined motor and pump. Concepts like the Innas Hydraulic Transformer are based on an axial piston pump whose valve plate has three instead of the common two openings connecting the ports to high pressure, tank pressure and transfomation pressure lines [3]. The novel booster concept proposed in this paper applies this working principle to pneumatics.
As air having a much lower viscosity than hydraulic fluids, an actuation of the cylinders using a valve plate would lead to very high leakage and therewith low efficiency of the booster. Therefore, a concept using a radial piston motor with actuation by switching and check valves is proposed.
Fig. 1 shows a schematic of this integrated pressure booster concept and the p-V-diagram of the cycle within one cylinder. The booster consists of three to six cylinders in radial layout. The pistons are connected through a crank drive with the crank length $l_{\mathrm{crank}}$ and the rod length $l_{\mathrm{rod}}$. Each

cylinder is actuated using two switching valves connecting the chamber to the pressure supply and the environment, respectively. Connection to the higher output pressure $p_{\mathrm{out}}$ is carried out via a check valve.

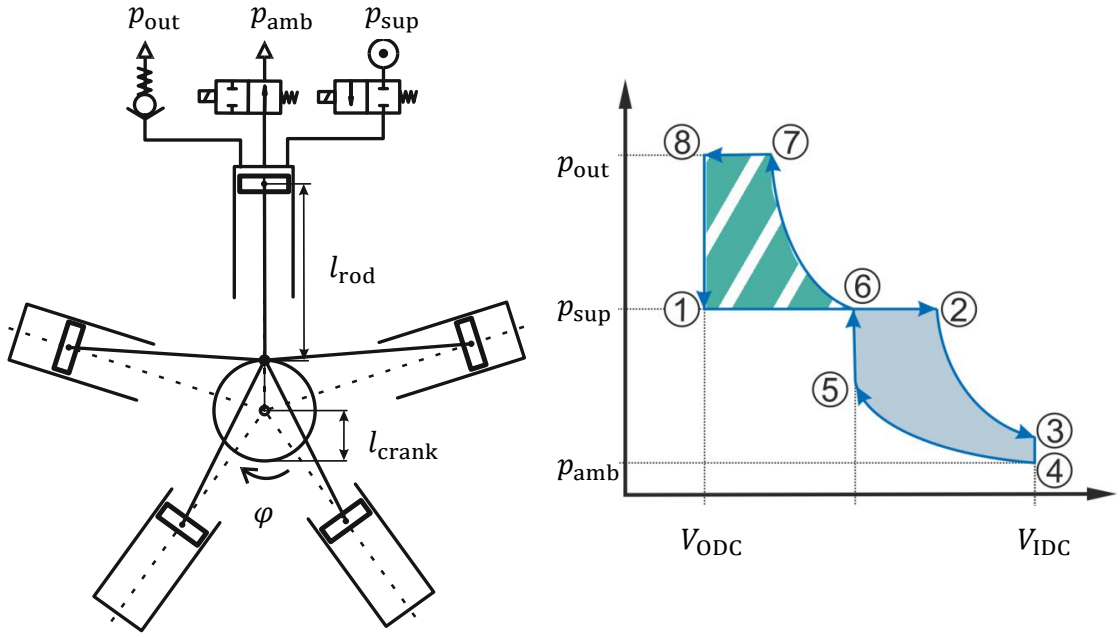


**Fig. 1:** Schematic and p-V-diagram of the integrated booster concept

At the beginning of the cycle, the piston is in the outer dead center (ODC) and the cylinder chamber is connected to the supply pressure $p_{\mathrm{sup}}$. The piston acts in motor mode. At a certain point during the piston stroke, the valve connecting the cylinder and the supply is closed to use the expansion energy contained in the air. When the piston reaches its inner dead center (IDC), the cylinder chamber is connected to the environment for a short period of time to exhaust the chamber. Now, both magnetic valves are closed and the air within the chamber is compressed. This reduces the air mass added to the chamber between points 5 and 6 in the p-V-diagram. At point 5, the supply valve opens briefly and the cylinder chamber is filled with supply air again. The valve closes at point 6, and the compression cycle starts. When the pressure in the chamber reaches the outlet pressure of the booster (point 7), the check valve opens and the air is pushed out. At the ODC (point 8), the check valve closes again due to the pressure drop caused by the forced piston movement and the cycle restarts. In an optimal booster cycle, the work of the motoring cycle (solid blue area in the p-V-diagram) equals the work needed to conduct the compression cycle (green dashed area).
In a simulation study the number of cylinders of the unit, the bore size and stroke length as well as the ratio between supply and outlet pressure are varied. The influence of these parameters on the overall efficiency of the transducer is examined. The switching points of the valves considerably influence the efficiency of the booster. Therefore, an optimization of these points is carried out.
Additionally, losses caused by friction between piston and cylinder as well as leakage are evaluated and their influence on the overall efficiency is identified.
To allow a comparison of the efficiency at different pressure levels and pressure ratios, the thermodynamic concept of exergy is used to assess the efficiency of the different configurations (see e.g. [4]).

### 2.1 Configurations

Different configurations of the booster were examined in the simulation study to obtain a good knowledge of the main impact on the efficiency. This includes the number and size of the cylinders as well as the leakage mass flow between the pistons and the cylinder wall.
Table 1 shows an overview of the 9 different pressure transducer configurations that were examined in the study. Off-the-shelf radial piston motors were taken as basis for the geometrical values. This includes configurations 1, 2 and 5. Additionally, scaled versions were simulated as well. Configuration 4 represents a five cylinder motor with the piston diameter and lengths of configuration 1. Configurations 3, 6 and 9 were obtained by scaling the piston diameter, rod length and crank length of the smaller builds 1, 4 and 7. Configurations 7 to 9 represent a six cylinder version, which corresponds to two of the three cylinder motors mounted on a single shaft.

**Table 1:** Overview over the different configurations examined in the study

| Configuration | Number of cylinders | Piston diameter | Crank length | Length of connecting rod | Angle between 2 cylinders |
|---|---|---|---|---|---|
| 1 | 3 | 22 mm | 7 mm | 56 mm | 120° |
| 2 | 3 | 32 mm | 9.25 mm | 61.25 mm | 120° |
| 3 | 3 | 44 mm | 14 mm | 112 mm | 120° |
| 4 | 5 | 22 mm | 7 mm | 56 mm | 72° |
| 5 | 5 | 32 mm | 9.25 mm | 61.25 mm | 72° |
| 6 | 5 | 44 mm | 14 mm | 112 mm | 72° |
| 7 | 6 | 22 mm | 7 mm | 56 mm | 60° |
| 8 | 6 | 32 mm | 9.25 mm | 61.25 mm | 60° |
| 9 | 6 | 44 mm | 14 mm | 112 mm | 60° |

## 3. Simulation model

To examine the efficiency of the different configurations, a simulation model was implemented in the lumped parameter simulation environment DSHplus. This includes mathematical models for the pistons and the actuation by valves as well as the kinematics of the crank shaft.

### 3.1 Mathematical description

Fig. 2 shows a schematic of one cylinder including the crank drive which converts the linear movement of the piston into a rotational movement of the shaft.

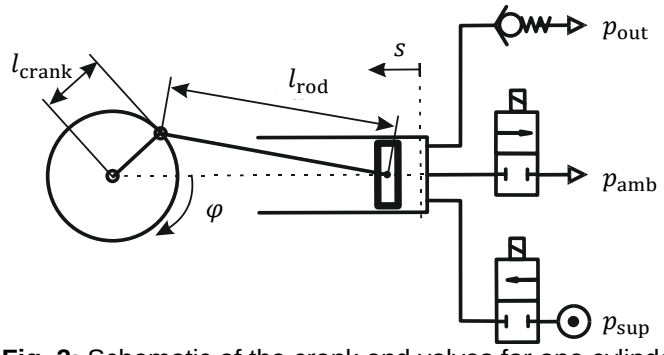


**Fig. 2:** Schematic of the crank and valves for one cylinder

The crank length $l_{\mathrm{crank}}$ and the length of the piston rod $l_{\mathrm{rod}}$ and their ratio $\lambda_s = \frac{l_{\mathrm{crank}}}{l_{\mathrm{rod}}}$ have a large influence on the dynamic behaviour of the booster. The piston position $s(\varphi)$ and the piston velocity $\dot{s}(\varphi)$ can be estimated using the equations (1) and (2) for $\lambda_s^2 \ll 1$, which is valid for all configurations examined in the study.

$$s(\varphi) = l_{\mathrm{crank}} \cdot \left[1 - \cos(\varphi) + \frac{1}{4} \cdot \lambda_s \cdot (1 - \cos(2\varphi))\right] \tag{1}$$

$$\dot{s}(\varphi) = \frac{ds(\varphi)}{dt} = \frac{ds(\varphi)}{d\varphi}\omega = l_{\mathrm{crank}} \cdot \omega \cdot \sin(\varphi) + \frac{1}{2} \cdot \lambda_s \cdot \sin(2\varphi) \tag{2}$$

The torque applied on the shaft by each piston depends on the angular position and the pressure in the cylinder chamber. The torque $M_{\mathrm{press}}$ applied by each piston can be calculated by equation (3) using the pressure force $F_{\mathrm{G}} = \Delta p \cdot A_{\mathrm{piston}}$ with $\gamma = \arcsin\left(\frac{l_{\mathrm{crank}}}{l_{\mathrm{rod}}} \cdot \sin\varphi\right)$.

$$M_{\mathrm{Press}} = F_{\mathrm{TG}} \cdot l_{\mathrm{crank}} = \frac{\cos(90° - \varphi - \gamma)}{\cos\gamma} \cdot F_{\mathrm{G}} \cdot l_{\mathrm{crank}} \tag{3}$$

Using the conservation of angular momentum leads to equation (4) for the calculation of the angular acceleration.

$$\sum_{i=1}^{n=n_{\mathrm{piston}}} M_{\mathrm{press},i} - M_{\mathrm{load}} = J_{\mathrm{Mot}} \cdot \ddot{\varphi} \tag{4}$$

These equations form a kinematic model of the booster from which the compression and expansion during the cycle can be derived. The change of pressure inside each chamber is calculated according to equation (5). Therein $\dot{p}_{\dot{m}}$ represents the pressure change by mass transfer, $\dot{p}_{\mathrm{HE}}$ represents the pressure change by heat exchange with the environment and $\dot{p}_{\dot{V}}$ represent the pressure change by volume change. [5]

$$\dot{p} = \dot{p}_{\dot{m}} + \dot{p}_{HE} + \dot{p}_{\dot{V}} \tag{5}$$

The mass flow in and out of each chamber is calculated within the valves. Leakage losses between the cylinder chambers are considered as well (cf. paragraph 4.3). To calculate the heat exchange between air and cylinder walls, a heat transfer coefficient of $\alpha = 3\frac{\mathrm{W}}{\mathrm{m^2K}}$ is assumed. The change of chamber volume is calculated with the axial piston velocity (eq. (2)).

### 3.2 Exergy efficiency

To assess the efficiency of the novel booster concept, the thermodynamic concept of exergy is used. The concept of exergy allows the comparison of different forms of energy. Exergy describes the ability to conduct work of different forms of energy when brought into equilibrium with the environment. As described by Krichel in [6], this is advantageous for the efficiency assessment of pneumatic systems.

According to equation (6), the exergy of an air mass flow can be calculated from its specific enthalpy $h$ and its entropy $s$. [7]

$$\begin{aligned}\dot{E}_{\mathrm{air}} &= \dot{m}_{\mathrm{air}} \cdot \Big(h(T_{\mathrm{air}}) - h(T_{\mathrm{amb}}) - T_{\mathrm{amb}} \cdot \big(s(T_{\mathrm{air}}, p_{\mathrm{air}}) - s(T_{\mathrm{amb}}, p_{\mathrm{amb}})\big)\Big) \\ &= \dot{m}_{\mathrm{air}} \cdot \left[c_{\mathrm{p,air}} \cdot (T_{\mathrm{air}})\right]\end{aligned} \tag{6}$$

The exergy efficiency can be calculated as the ratio between the exergy flow $\dot{E}_{\mathrm{out}}$ out of the booster and the exergy flow $\dot{E}_{\mathrm{in}}$ fed to the booster (caf. equation (7)) subsequently.

$$\xi = \frac{\dot{E}_{\mathrm{out}}}{\dot{E}_{\mathrm{in}}} \tag{7}$$

Assuming an isothermal change of state between the inlet and the outlet of the booster leads to equation (8) for the exergy efficiency of the booster. This assumption is valid for the whole booster system if the output air flow is fed into an accumulator where it cools down to ambient temperature.

$$\xi = \frac{\dot{m}_{\mathrm{out}} \cdot \ln\left(\frac{p_{\mathrm{out}}}{p_{\mathrm{amb}}}\right)}{\dot{m}_{in} \cdot \ln\left(\frac{p_{\mathrm{in}}}{p_{\mathrm{amb}}}\right)} \tag{8}$$

This definition of the exergy efficiency is used throughout the simulation study presented in paragraph 4.

### 3.3 Implementation in DSHplus

Fig. 3 shows an excerpt of the simulation model implemented in DSHplus for one cylinder. The cylinder creates a force on the thrust crank which represents the connecting rod and the excentricity of the crank shaft. Within the crank, the torque built up by each cylinder is calculated.

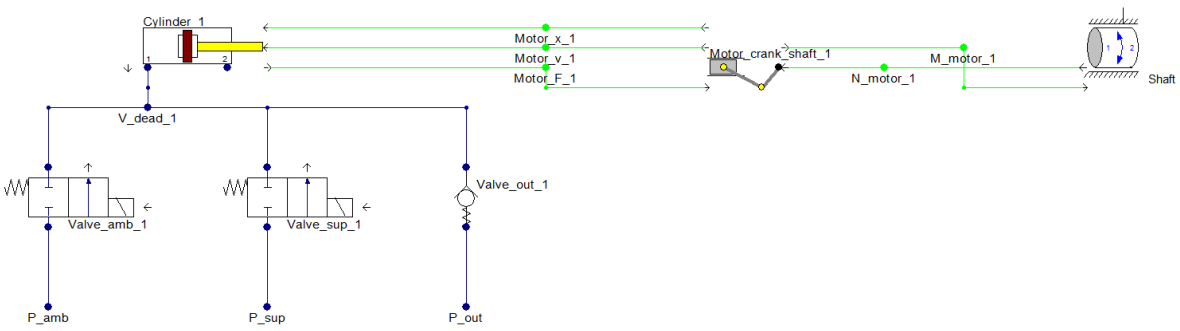


**Fig. 3:** Excerpt of the simulation model for one cylinder

The torque leads to an acceleration of the rotating mass ("Shaft") on the right hand side of Fig. 3. Therewith, the rotational position and speed are calculated and fed back to the crank where they are transmitted into the position and velocity of the cylinder.
In dependence on the rotational position of the shaft, the valves connecting the cylinder chamber to the environment and the pressure supply are switched. The check valve to the high pressure outlet opens automatically at a pressure difference of 0.1 bar. To gain maximum efficiency, the switching points of the 2/2-way-valves are varied for each configuration and have to be adapted to the pressure ratio between supply and target pressure. The opening and closing time of the valves is 10 ms which is in the range of typical fast switching valves.

## 4. Results

In the following section, some exemplary results of the simulation study are shown. To illustrate the process in one cylinder chamber, fig. 4 shows the valve signals for both switching valves for one cylinder in comparison to the normalised piston stroke. Additionally, the chamber pressure and the output mass flow through the check valve connecting the chamber to the output volume are shown.

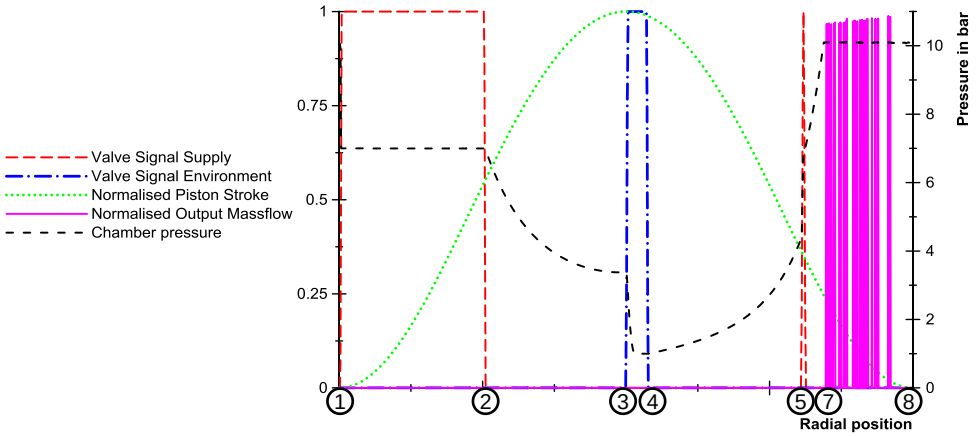


**Fig. 4:** Valve signals, piston stroke, output massflow and chamber pressure for one cylinder during one load cycle

As long as the supply valve is open (between points 1 and 2), the chamber pressure equals supply pressure (here: 7 bar). At point 2, the valve closes and the pressure decreases while the piston keeps on moving out until it reaches its inner dead center at point 3 where the valve to the environment opens. Now, the chamber is exhausted and the pressure falls to ambient pressure. Closing the valve at point 4 starts the precompression of the air volume inside the chamber. At point 5, the supply valve opens again for a brief period of time and the chamber is filled with air at supply pressure. The angular position of point 5 is subject to optimisation so that the amount of work executed during motoring and the energy needed by the compression are adjusted. The air inside the chamber is compressed, until the output pressure (here: 10 bar) is reached at point 7. Now, the air inside the chamber is pushed out through the check valve. This causes a pressure drop in the chamber which leads to closing of the check valve. Due to its small opening pressure in combination with a relatively high conductance the check valve opens and closes in a high frequency which shows in strong oscillations of the output mass flow.
Dependent on the supply and output pressure, the switching points of the supply valve have to be altered to gain maximum efficiency. Filling the chamber for a longer period of time increases the maximum output pressure and the maximum output mass flow because the mean driving torque increases. On the downside, more supply air is needed, which lowers the efficiency. Later refilling of the chamber during outward movement decreases the high pressure output because a smaller volume is filled with air at supply pressure and therewith, less air mass is compressed. A longer connection to the environment lowers the driving torque needed, as the mean pressure during outward movement decreases. Due to the smaller amount of precompressed air, the air mass

which has to be filled to the chamber during the second opening of the supply valve increases. All these different impacts have to be considered to gain maximum efficiency.
Automatic optimisation of the switching points would require a closed loop control concept for the booster considering the input and output pressure as well as the rotational speed. In the study presented here, no such concept was implemented. Instead of mathematical optimisation, iterative adjustment of the switching points was executed for each load and booster configuration.
Fig. 5 shows the p-V-diagram for the pressure build up phase for a three piston booster in comparison to a six piston configurations. Both configurations feature the same piston diameter.

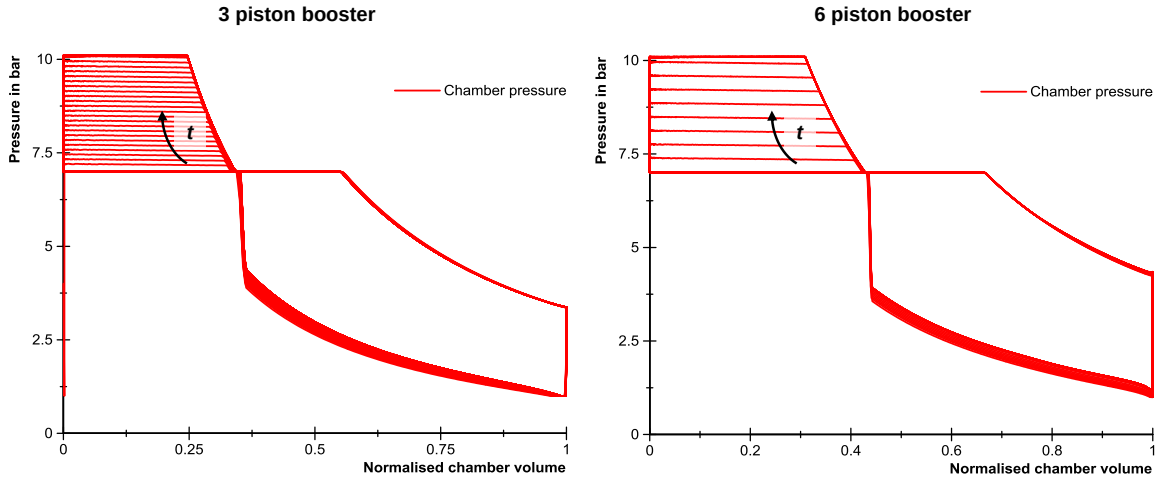


**Fig. 5:** Comparison of p-V-diagrams for 3- and 6-piston booster

The output pressure rises with each rotational cycle which is to be seen in the lines in the upper part of the diagram. Due to the lower cylinder number, the smaller booster needs a higher number of revolutions to reach the pressure of 10 bar in the accumulator. In the simulations shown in fig. 5, the switching points for the valves controlling the motoring cycle and the start of the compression cycle have been adapted to the load for maximum performance. This leads to different switching points for the three and six piston booster.

### 4.1 Influence of the piston diameter and cylinder number

Results of the different simulations show, that the efficiency of the booster increases with the piston diameter when all other parameters are kept constant. The maximum exergy efficiency is 60.5 % for the scaled geometry in a six-cylinder-configuration.
Table 2 and fig. 6 show exemplary results of the simulation study for the different configurations explained in table 1. These show a large influence of the number of cylinders. Especially the dynamic behaviour of the booster differs between the different configurations. A larger number of cylinders reduces the fluctuations in driving torque at the shaft which leads to a smoother rotation.

**Table 2:** Results of the simulation study

| Confi-guration | Maximum Efficiency | No. of Revolutions until $p_{max}$ is reached | Annotations |
|---|---|---|---|
| 1 | 21.5 % | 86 | Bad dynamic behaviour |
| 2 | 45.0 % | 22 | Bad dynamic behaviour |
| 3 | 45.8 % | 10 | Bad dynamic behaviour |
| 4 | 32.5 % | 37 | High fluctuation in rotational speed |
| 5 | 42.0 % | 11 | High fluctuation in rotational speed |
| 6 | 59.9 % | 4 | High fluctuation in rotational speed |
| 7 | 29.4 % | 30 | |
| 8 | 42.8 % | 8 | |
| 9 | 60.5 % | 2 | |

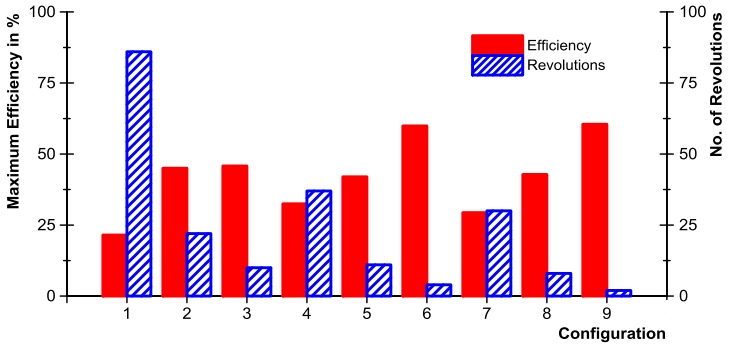


**Fig. 6:** Maximum exergy efficiency and number of revolutions needed to reach output pressure for the different configurations

Additionally, the number of revolutions needed until the desired maximum pressure in the output volume is reached, decreases with the number of cylinders as well as with the piston diameter. An increase in piston diameter is beneficial for the efficiency, because friction and leakage losses have a lower impact in comparison to the driving torque and mass flow in and out of the cylinder chamber.

### 4.2 Sensitivity on valve switching points

The sensitivity of the exergy efficiency on the valve switching points is examined in the following section. Fig. 7 shows a comparison of three p-V-diagrams for configuration 9 (6 pistons, 44 mm piston diameter). The air supply during motoring mode is switched off at three different rotational positions of the crank shaft: 91°, 95° and 100°. Due to the kinematics of the motion, this leads to a relatively large difference in the chamber volume filled with air at supply pressure. Therefore, the chamber pressure $\Delta p_{\mathrm{IDC}}$ at the inner dead center shows a difference of around 0.6 bar.

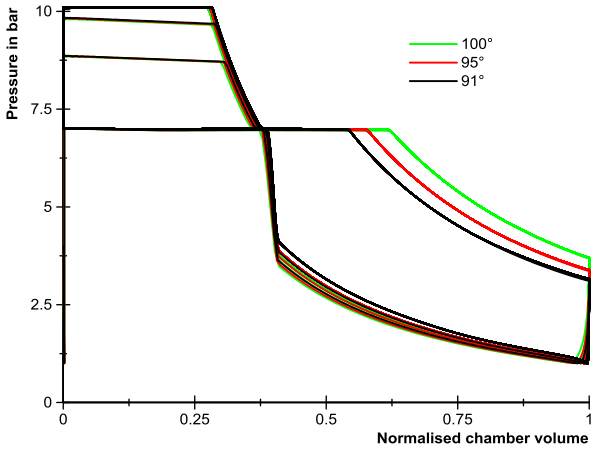


**Fig. 7:** Comparison of the p-V-diagrams for different switching points for the supply valve

The influence of the different switching points on the exergy efficiency of the booster is shown in fig. 8. It is obvious that later switching reduces the exergy efficiency by about 7 %.

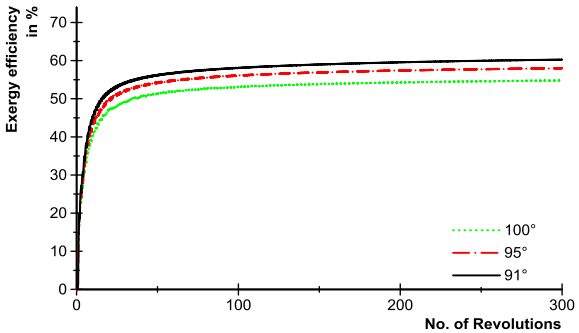


**Fig. 8:** Slope of the efficiency for different switching angles

Due to the smaller driving torque resulting from the lower mean pressure during the motoring cycle, it is not possible to reduce the angle at which the air is switched off infinitely. At a switching angle of 90°, the dynamics of the booster deteriorate and the booster frequently stops rotating. A higher driving torque also increases the rotating speed and therewith the output mass flow of the booster.

### 4.3 Sensitivity on leakage mass flow

The leakage between pistons and cylinder walls has large influence on the obtainable efficiency of the transformer. This is shown exemplarily for a six cylinder booster with large piston diameter (configuration 9 in Table 1) in Fig. 9. The conductances used to compute the shown diagram equal maximum gap heights of 9 µm, 11 µm and 19 µm, respectively.

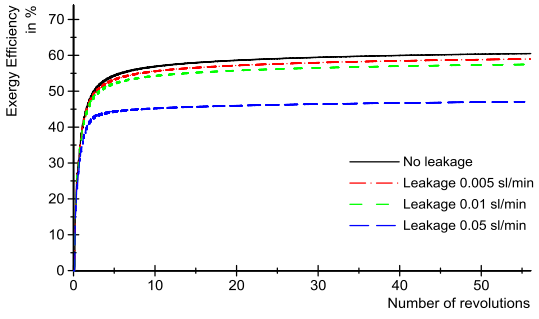


**Fig. 9:** Slope of the efficiency for different leakage flow coefficients

The higher the leakage flow, the lower the efficiency will be. Considering zero leakage the maximum efficiency of the booster is 60 % whereas a high leakage conductance reduces the efficiency to 47 %. If a conductance of 0.01 sl/min/bar is assumed, the total leakage mass flow equals 3.9 % of the supply mass flow or 8.5 % of the high pressure output flow. This is within the typical range for piston compressors (cf. e.g. [6]) and leads to a maximum efficiency of 57.5 % for the pressure transducer.

## 5. Conclusions & Outlook

A novel concept for pneumatic pressure boosters using radial piston motors is shown in the paper. These boosters have a large potential to increase the efficiency of local pressure adjustment in industrial applications if losses due to friction and leakage can be kept low. The simulation of the exergetic efficiency of the proposed booster concept shows results up to 60 %.
The influence of the switching points of the different valves is shown in one example. By adapting these switching points to the desired output mass flow and pressure, the efficiency can be kept high.
It is shown that especially the reduction of the leakage mass flow through the gap between the pistons and the cylinder wall has great influence on the efficiency. If the leakage flow increases, the efficiency decreases by far due to the larger amount of air which has to be supplied in motor mode as well as the lower amount of air discharged to the high pressure side.
In the next step, a working model of the integrated pressure transducer will be designed and built. Additionally, a different concept featuring two separate rotating units for motor and compressor mode working on a single shaft is currently under investigation at IFAS. A closed loop control concept for the automatic adaption of the switching points of the different valves may be developed to gain maximum efficiency depending on the output pressure and mass flow needed in industrial applications.

### Acknowledgements

The authors thank the Research Association for Fluid Power of the German Engineering Federation VDMA for its financial support. Special gratitude is expressed to the participating companies and their representatives in the accompanying industrial committee for their advisory and technical support.

### References

[1] Krichel, S., Gauchel, W., Kefer, J., Genauer hinsehen lohnt sich! Niederdruckpneumatik ist kein Garant für verbesserte Energieeffizienz, O+P Ölhydraulik und Pneumatik (in German language), 2014, pp. 20–27.
[2] Vukovic, M., Sgro, S., Murrenhoff, H.: STEAM – A Mobile Hydraulic System with Engine Integration. In: Proceedings of the ASME/BATH 2013 Symposium on Fluid Power & Motion Control FPMC2013 October 6-9, 2013, Sarasota, Florida, USA.
[3] Achten, P., van den Brink, T., Potma, J., Schellekens, M., Vael, G.: A four-quadrant hydraulic transformer for hybrid vehicles. In: The 11th Scandinavian International Conference on Fluid Power, SICFP'09, June 2-4, 2009, Linköping, Sweden.
[4] Merkelbach, S., Murrenhoff, H., et al.: Pneumatic or electromechanical drives – a comparison regarding their exergy efficiency. In: 10th International Fluid Power Conference (10th IFK). 8th - 10th March 2016, Dresden, Germany, 2016, pp. 103–115.
[5] Murrenhoff, H., Reinertz, O.: Fundamentals of fluid power – Part 2: Pneumatics, Shaker, 2014, Aachen, Germany.
[6] Krichel S. V., Sawodny O., Hülsmann S., Hirzel S. and Elsland R., 2012,"Exergy Flow Diagrams as Novel Approach to Discuss the Efficiency of Compressed Air Systems," *Proceedings of the 8th International Fluid Power Conference IFK*.
[7] Baehr H. D., and Kabelac S., 2012. *Thermodynamik*, Springer Berlin Heidelberg, Berlin, Heidelberg.